

# Heart Blockage Prediction Using Differential Equation with R-LOOKAHEAD- LSTM and DWARF Mongoose Optimization Based on Squeeze Net Method

Somasundaram Kuppusamy<sup>1\*</sup>, Sathish Kumar Rangasamy<sup>1</sup>, Sanjayprabu Sivakumar<sup>1</sup>,  
Karthikamani Ramamoorthi<sup>2</sup>

<sup>1</sup>Sri Ramakrishna Mission Vidyalaya College of Arts and Science, Coimbatore, Tamil Nadu, India.

<sup>2</sup>Sri Ramakrishna Engineering College, Coimbatore, Tamil Nadu, India

## Abstract

Huge diversity has evolved in the medical industry as a result of improved computer power and technology, particularly in the detection of cardiac occlusive disorders in humans. It has a devastating effect on human life and is now one of the worst cardiac illnesses in humans. To increase the model's capacity for prediction, this study suggests an optimization approach for dwarf mongoose and using differential Equation with R-Lookahead-LSTM-based cardiovascular disease prediction model. Using the R-Lookahead method, the long-term memory network model was further optimized. It is possible to enhance LSTM network models to demonstrate the model's propensity for speed and stability. This model can then be used to forecast cardiovascular disease. Additionally, we employ Squeeze Net adjusted using the R-Lookahead-LSTM-DMOA dwarf mongoose optimization method, which modifies several components of dwarf mongoose feeding to anticipate cardiovascular disease. This research includes a collection of ECG signal data from individuals with cardiac conditions. This unique dataset consists of 1937 individual patient records, all of which were gathered using an ECG Device. The data acquired comprises 12 leads-based ECG signal data. Additionally, according to the experimental findings, the R-Lookahead-LSTM-DMOA Squeeze Net method's highest accuracy is 0.867287, its precision is 0.846625, and its recall is 0.896720.

**Keywords:** Numerical Analysis; Optimization; Heart Blockage; Squeeze Net Approach

## 1. Introduction

Cardio-occlusive disease, the largest cause of fatalities globally, damages the heart's structure and function. Heart attacks, the most difficult kind of cardiovascular illness to treat, can result from a variety of cardio-occlusive diseases [1]. The heart, which circulates blood to the body's many organs, is the major component of the human body. The body's numerous organs will stop functioning if the heart isn't functioning correctly, and the individual will pass away. Consequently, it is crucial that the heart is operating properly. Cardio-occlusive disease is regarded as the leading cause of mortality worldwide [2]. Heart disease also affects men and women differently. Thus, the development of effective cardiac disease prediction methods will aid in lowering mortality [3, 4]. Heart disease diagnosis is a challenging challenge in medicine that frequently raises mortality. In order to do this, researchers have developed a technique for automated illness

detection that can detect cardiac problems. Researchers gather clinical data from clinical experience to diagnose cardiac illness and then confirm the diagnosis using diagnostic techniques and medical diagnoses [1].

Emerging sectors like cloud computing, big data, artificial intelligence, and the Internet of Things are flourishing as the global information technology revolution enters a new phase of growth. Additionally, technology has given old sectors a fresh lease of life as they evolve and change. It is now being steadily implemented in a number of economic sectors, including transportation, logistics, and education. The medical profession will progressively advance from the traditional medical and health business to the stage of smart medical care as a result of the ongoing accumulation of medical data. At this point, the speed at which computers can process data has multiplied thousands of times, significantly enhancing the use cases for artificial intelligence in

the medical and health sector. These use cases include illness prediction, medication research, medical picture analysis, and record analysis. The Internet of Medical Things is one of several reasons that encourage the growth of patient-centric medical data networks [1, 2]. Machine learning, the primary approach of artificial intelligence research, has made significant advancements along with the recent spectacular expansion of AI. It has produced exceptional outcomes in the areas of voice recognition, risk analysis, and illness detection. It offers a fresh study avenue for illness prediction and has high prediction accuracy.

Scale model effectiveness has to be verified. Acute coronary and sealing [6] et al. employ a variety of basic research models, including the early basic research model, the basic analytical model, the basic mechanical research model, hemorrhagic heart disease [3], liver disease [4], the basic disease model, and the Japanese scale model for diagnosis. In the first illness prediction model, machine learning methods are mostly used to construct the prediction model. Researchers now need to employ machine learning algorithms to construct illness prediction models in order to increase the precision and efficacy of disease prediction. Reference [7] offers a hybrid method based on multivariate adaptive regression splines and random forests for creating illness prediction models.

In this proposed work, we explore a novel model and outline an approach for cardiac disease prediction using ECG signal data. Here, missing data replacement and quantile normalization are used in the pre-processing of the input data. Using feature selection, columns of pre-processed data are processed to choose pertinent features based on Kumar-Hassebrock similarity and the coefficient of agreement. Heart disease is predicted by SqueezeNet, taught by DMOA using SqueezeNet weights, and detected by DMOA as normal or abnormal patients. Here are the work contributions we've suggested.

- Deep learning networks for heart disease early detection.
- Compare the planned work to current cutting-edge techniques.

- Offers real-time implementation of advised techniques.
- A range of outcome indicators, including as accuracy, precision, recall, and F1-score, can be used to assess your competency.

The structure of this work is as follows: In Section 2, the relevant studies in the area of heart disease prediction were evaluated. The model is defined in Section 3. Results and discussion in Section 4 demonstrate the effectiveness of the suggested effort. In Section 5, the research's conclusion is detailed.

## **2. Objectives**

The strategies for predicting heart disease are listed below. For the purpose of identifying cardiac illness, Cora et al. [20] created BF-PSO (Bacterial Foraging Particle Swarm Optimization). Here, BFO (Bacterial Foraging Optimization) and PSO are combined to create a hybrid (Particle Swarm Optimization). The suggested model increases detection accuracy by removing more pertinent characteristics, but it requires the most training time. [4] Bidirectional long short-term memory is modelled using Bi-LSTMCRF (Conditional Random Field) to forecast cardiac disease. Here, we employ a bidirectional LSTM to analyse medical data and a CRF model to calculate the association between different characteristics. This approach has the highest computational cost. The XG Boost model for cardiac diagnostics was introduced in [21]. Complex datasets, however, cannot be handled by this methodology. Heart disease prediction using a regression learning-based neural network classifier (RLNNC) was created in [1]. Despite offering superior detection outcomes, this technique requires more computing resources including blood sugar, cholesterol, chest discomfort, gender, age, blood pressure (BP), etc. For diagnosis in ANFIS, we employ gradient-based learning and recurrent learning techniques, however there is a chance that we will become mired in local problems.

Many machine learning algorithms have been developed for CVD detection in addition to human methodologies. It has been investigated how to categorize the key indicators of cardiac disease [19]. There are seven algorithms used for classification: NB, KNN, LR, DT, NN, SVM, and Vote.

You may access the Cleveland dataset from the UCI Machine Learning Repository, which has 303 objects and 76 characteristics. Tenfold cross-validation is used to train and test the model. 10 fold cross-validations were utilized. This is because there aren't many training instances in the dataset, and employing data splits like train-test splits might cause the prediction performance of the model to be underestimated because there aren't many samples in the training set. But with 10-fold validation, 90% of the data are available for the model to learn from. The voting classifier's accuracy was greater, at 87.4%.

A heart disease risk prediction model that uses feature selection and ensemble classification techniques. Electronic studies have shown that ensemble methods like as bagging and boosting, can improve the predictability of poor classifiers and the risk of heart disease. The inclusion of feature selection significantly improves prediction accuracy [7].

### 3. Methods

#### 3.1 Aim

To increase the model's capacity for prediction, we suggest an optimization approach for dwarf mongoose and using differential Equation with R-Lookahead-LSTM-based cardiovascular disease prediction model by employing the ECG signal data of individuals with cardiac conditions.

#### 3.2 Design

We design the proposed method using R-Lookahead method, LSTM-DMOA and SqueezeNet. Additionally, we employ Squeeze Net adjusted using the R-Lookahead-LSTM-DMOA dwarf mongoose optimization method, which modifies several components of dwarf mongoose feeding to anticipate OCD.

#### 3.3 Dataset Description

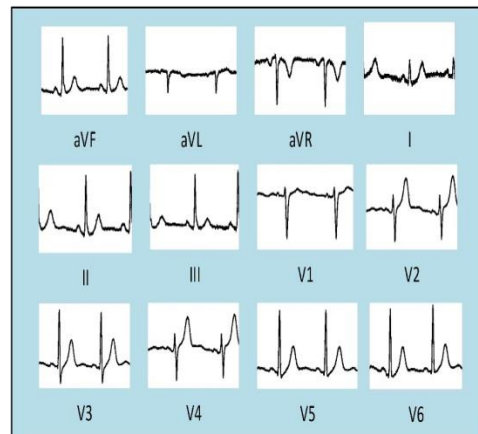


**Figure. 1 Typical 12-lead ECG signals of a healthy individual**

A set of 12-lead standard ECG signal data was gathered from various cardiac institutes across Pakistan, each originating from different patients. These ECG signal data have been carefully anonymized, ensuring that no personal information about the patients is included. To ensure accuracy, multiple medical experts have annotated all the ECG signal data. Table 1 presents the distribution of images among different cases. The ECG data was captured using an EDAN SE-3 series 3-channel ECG machine with a sampling frequency of 500 Hz. After acquisition, the data was subjected to processing using either a 0.67–25 Hz band-pass filter (BPF) or a 0.5–100 Hz BPF along with a 50 Hz notch filter to remove noise. Then, the 12 standard ECG lead printouts (Figure 1) were generated for analysis. The generated model received its input from these processed photos.

**Table 1. Dataset [26] Details**

Category	No. of Distinct ECG Images
Normal Person ECG Images	859
Myocardial Infarction Patient	77
Patients with Previous History of Myocardial Infarction	203
Patients with Abnormal Heartbeat	548

#### 3.4 Setting of Study

This study shows one fast and one slow set of weights are that maintained by the Look ahead algorithm. The proposed method employs the R-Lookahead algorithm to enhance and optimize the LSTM model and suggests an R-Lookahead-LSTM model for the prediction of cardiovascular illness. LSTM-DMOA can develop and enhance potential

solutions for a particular optimization issue. DMO tunes with just one parameter. In this approach, a pygmy monkey moves between different areas of the problem search space in quest of food. SqueezeNet often comprises of a variety of free modules, such as dilation layers and squeezed convolutional layers. The squeeze convolutional layer's output is forwarded to the next enhancement layer in the free module. In addition, Squeeze Net begins with a first convolutional layer that is monitored independently by eight separate modules and finishes with a final convolutional layer. Correlation a type of statistical analysis is used in the proposed method.

### 3.5 Pre-processing

To improve the quality of the data, different treatments were applied to the ECG printouts. The printouts were first separated into several areas reflecting the 12-lead ECG curves, shown in black on a white backdrop, after noise was eliminated using filtering. Using thresholding procedures based on the green (G) channel of the ECG pictures and morphological processes, respectively, further stages comprised removing background gridlines and binary noise [27].

Based on the dimensions of the area of interest for each ECG lead on the printout, rectangular non-overlapping windows of various widths were selected to accommodate for differences in spatial resolution across patients. For heart disease subjects, window sizes of  $112 \times 112$ ,  $189 \times 189$ , and  $315 \times 315$  were used, while for normal subjects, a window size of  $112 \times 112$  was employed [27]. These windows were manually positioned on the 12-lead ECG printout. All ECG segments were then resized to  $100 \times 100$  for input into the subsequent network analysis.

### 3.6 Proposed System Model for Predicting Disease using Ode with R-Lookahead - LSTM

The population under consideration may have an incidence rate of illness of  $i$ , an age-specific mortality rate of  $m_1$  while ill, and an absence of disease death rate of  $m_0$ .  $S$  (susceptible) and  $C$  (cases) stand for the numbers of both affected and unaffected people, respectively. Assume that  $S$  and  $C$  are two sufficiently big integers to be regarded as continuously differentiable functions. As was said in the Introduction, disease-death models only need one time variable, age  $a$ , with a

$a_0 = 0$ , to represent temporal changes in populations. The rate of change of the  $S$  and  $C$  values in disease-free and sick people, respectively, is thus described by the system of ordinary differential equations provided by (1) and (2).

$$\frac{dS}{da} = -(i + m_0) \quad (1)$$

$$\frac{dC}{da} = iS - m_1 C \quad (2)$$

Given the ODE's straightforward form and the  $m_0$  and  $m_1$ . Age-specific morbidity and death rates, respectively. The ODE model has an additional condition that constitutes a well-known disease-death model and a person with an undiagnosed disease. The numbers  $N_j$ ,  $j = 0, 1, 2$ , as well as the transition rates depend on the calendar time  $t \in \mathbb{R}$  and on the age  $a$ ,  $a \in [0, \infty)$ .  $N_j(t, a)$  denotes the number of people in state  $j$ ,  $j = 0, 1, 2$ , aged  $a$  at time  $t$ . Assuming no movement,  $N_j$  is the year of the next system of partial differential equations (ODE), then Equation (3) can be written as

$$\begin{aligned} (\partial_t + \partial_a) N(t, a) &= -(\mu_0(t, a) \\ &+ \lambda_0(t, a)) N_0(t, a) \end{aligned}$$

In this part, we enhance the LSTM model by replacing the Tanh activation features in the input gates with Softmax activation features, which helps the model to converge more quickly. Figure 2 depicts the updated LSTM model structure.

The updated LSTM's four primary processing phases are as follows:

Step 1: Don't forget to alter any outdated information that has to be deleted from the cell state using the gate's sigmoid activation function. The forget gate selects how much to retain the output vector  $f_t$  of the previous neuron state  $C_{t-1}$  and outputs  $h_{t-1}$  from the previous hidden layer state and the current input  $x_t$  as input. It goes like this:

$$f_t = \sigma(W_f \cdot [h_{t-1}, x_t] + b_f) \quad (4)$$

Step 2: Enter how much more information the gate reveals about the condition of the cell. The hidden layer state output  $h_{t-1}$  from the previous instant and the current input decide which data is inserted first. The input gate changes each component of the candidate cell state  $C_t$  from 0 to 1 and modifies the amount of extra information given by the network after receiving  $C_t$  from the Soft sign network layer through  $h_{t-1}$  and  $x_t$ .

$$i_t = \sigma(W_i \cdot [h_{t-1}, x_t] + b_i) \quad (5)$$

$$\bar{C}_t = \text{Softsign}(W_c \cdot [h_{t-1}, x_t] + b_c) \quad (6)$$

The cell state data  $C_{t-1}$  is modified in step 3 to produce the new cell state data  $C_t$ . The updating algorithm is:

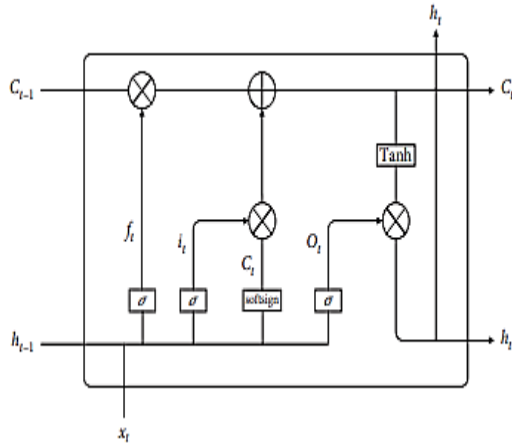


Figure 2: Improved LSTM model structure diagram

$$C_t = f_t * C_{t-1} + i_t * \bar{C}_t \quad (7)$$

Step 4: Calculating the output value of  $h_t$  is the responsibility of the output gate. After data has passed through the output gate, use  $h_{t-1}$  and  $x_t$  to assess the system's state. After using the Tanh function to resize the vector, add  $C_t$ . Finally, we obtain the present neural network's unit output. The equation is:

$$o_t = \sigma(W_o \cdot [h_{t-1}, x_t] + b_o) \quad (8)$$

$$h_t = o_t * \text{tanh}(C_t) \quad (9)$$

Eight sets of parameters, comprising four sets of weights ( $w_f$ ,  $w_t$ ,  $w_o$ , and  $w_c$ ) and four sets of bias items ( $b_f$ ,  $b_i$ ,  $b_o$ , and  $b_c$ ), should be taught to the LSTM model during training. Please use  $f_t$ ,  $i_t$ ,  $o_t$ , or  $C_t$ . Training sessions consist of:

Initialize the weight settings in Step 1

Step 2: Determine each neuron's forward output value using the aforementioned procedure.

Step 3: Reverse-calculate each neuron's error value.

Step 4: Based on the corresponding error value, calculate the slope of each weighting parameter.

Step 5: We update the weights using the R-Lookahead optimization method, iterate until the error reaches a preset threshold, and then the training is completed.

### 3.7 Enhancing the Lookahead Algorithm

To move closer to the ideal value or finally minimize the loss function, the LSTM must

continuously solve and update the weight and bias components of the model. In this chapter, we optimize the LSTM model (R-Lookahead algorithm) using the extended Lookahead optimization approach. One fast and one slow set of weights are maintained by the Lookahead algorithm. By adjusting the degree of deformation using a modified adaptive moment estimate approach, this component is made better in the quick weighting section. The first training phase may be completed rapidly because to the RAdam method's ability to dynamically turn on and off the adaptive momentum, which also prevents the severe oscillation issue brought on by the limited sample population. In Method 1, the R-Lookahead algorithm is shown.

### ALGORITHM 1: R-Lookahead algorithm

```

R-Lookahead algorithm
Require: Initial parameters  $\phi$ , objective function L
Require: Synchronization period k, slow weights step size  $\alpha$ , optimizer RAdam
for  $t = 1, 2, \dots$  do
  Synchronize parameters  $\theta_{t,0} \leftarrow \phi_{t-1}$ 
  for  $i = 1, 2, \dots, k$  do
    Sample minibatch of data  $d \sim D$ 
     $\theta_{t,i} \leftarrow \theta_{t,i-1} + \text{RAdam}(L, \theta_{t,i-1}, d)$ 
  end for
  Perform outer update  $\phi_t \leftarrow \phi_{t-1} + \alpha(\theta_{t,k} - \phi_{t-1})$ 
end for
return parameters  $\phi$ 

```

### 3.8 The disease prediction model R- Lookahead-LSTM

The LSTM approach, which is largely used in this section, may help to some degree with the gradient explosion and gradient disappearance issues that arise during the learning process for RNN models. The model structure of LSTM technology is improved and optimised using the RNN algorithm's model structure as a foundation. The RNN algorithm determines the input, forget, and output gates for each neuron. LSTM technology, however, considerably reduces the RNN algorithm's long-term need for data samples. However, the training results still show local optima in certain application scenarios, independent of the optimisation and

reconstruction methods used, due of the basic nature of the neural network model. The R-Lookahead algorithm is used in this chapter to improve the LSTM model and propose an R-Lookahead-LSTM model for the prediction of cardiovascular disease while taking into consideration the aforementioned problems. Algorithm 2 shows the steps involved in creating the model, and Figure 3 shows the workflow for the R-Lookahead-LSTM model.

**ALGORITHM 2: R-Lookahead-LSTM algorithm.**

Processing the data, looking for correlations in the data, utilizing the random forest technique (an ensemble learning algorithm) to choose features from the data, and figuring out the feature vectors required to create the model are the initial steps.

Step 2: Divide the previously processed data set in half, 7:3, into a training set and a test set.

LSTM model structure, number of network layers, and initialization parameters of the data samples in the training set are all determined by empirical testing in step three.

Step 4: After model training, use the R-Lookahead optimization technique to enhance the LSTM model's loss function.

Step 5: Assess the R-Lookahead-LSTM illness risk prediction model's ability to forecast outcomes using the test set data sample as input data.

Step 6: Utilize a variety of measures to assess the model's prediction effectiveness, including accuracy, recall, F1 score, specificity, and MCC value.

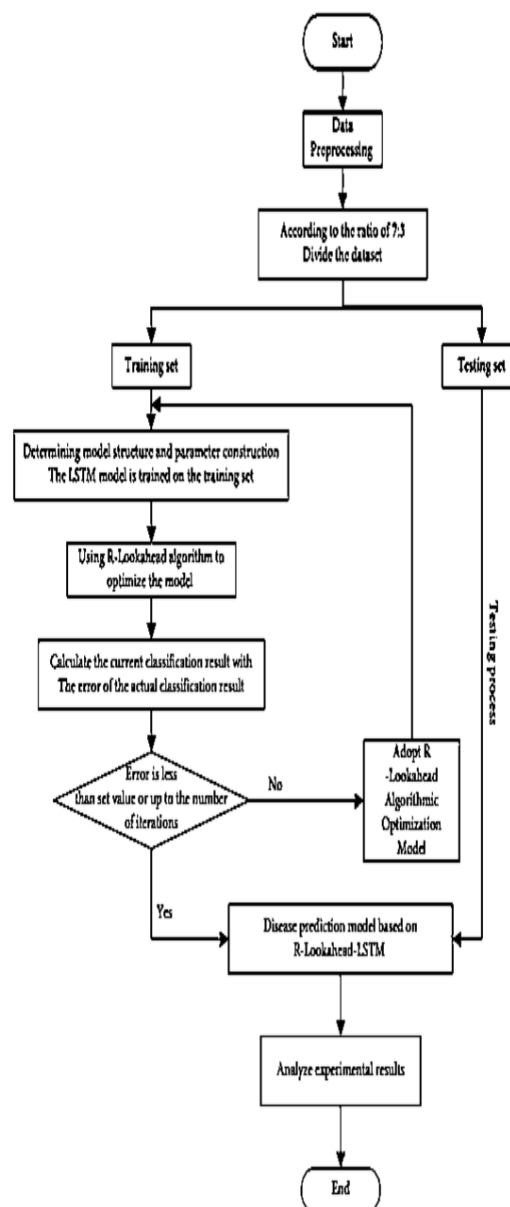
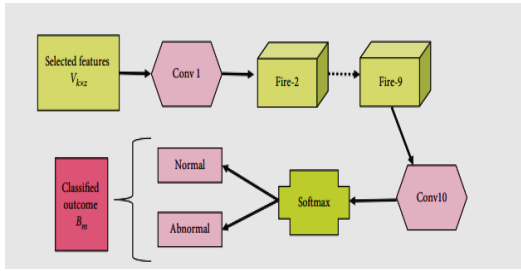


Figure 3: Flowchart for an R-Lookahead-LSTM-based illness prediction model

**4. Dwarf Mongoose Ptimization**

**4.1 Structure of SqueezeNet**

SqueezeNet often comprises of a variety of free modules, such as dilation layers and squeezed convolutional layers. The squeeze convolutional layer's output is forwarded to the next enhancement layer in the free module. In addition, SqueezeNet begins with a first convolutional layer that is monitored independently by eight separate modules and finishes with a final convolutional layer. First, Bm stands for the output of the SqueezeNet model. Max pooling is likewise carried out by SqueezeNet in two phases, as seen in Figure 4.



#### 4. Squeeze Net Training using DMOA

The DMOA described in this section was utilized to train the SqueezeNet employed in this investigation. The idea for DMOA is based on the dwarf mongoose's foraging characteristics. A metaheuristic paradigm for dealing with optimization complexity is DMOA [24]. DMOA can develop and enhance potential solutions for a particular optimization issue. In this approach, a pygmy monkey moves between different areas of the problem search space in quest of food. Additionally, DMO tunes with just one parameter. The following is a description of the DMOA algorithm's stages.

- (1) Initialization in order to provide an ideal solution, algorithmic restrictions and solutions are initialized in the first step.
- 2) Fitness evaluation. The following formula is used to choose the optimal solution based on the MSE.

$$b_{\min} = \frac{1}{w} \sum_{m=1}^w (B_m^* B_m)^2 \quad (10)$$

Where  $w$  denotes the overall sample count and  $B^*m$  the prediction or SqueezeNet classification outcome.

- (3) Alpha Group the population is initialized before calculating the overall solution efficiency. The probability values computed as follows are used to choose alpha females at this stage.

$$k = \frac{(b_{\min})_p}{\sum_{p=1}^t (b_{\min})_p} \quad (11)$$

Where  $t$  indicates how many mongooses there are for  $k$ , and  $b_{\min}$  indicates the fitness function. This is the solution upgrade approach:

$$s_{p+1} = s_p + \alpha_p * Q \quad (12)$$

Here,  $p$  stands for the random number distribution,  $Q$  stands for the heroine's words, which support the family, and  $s_p$  stands for the iteration's answer. After each repetition, the sleep mount is calculated and is given as follows:

$$L_r = \frac{(b_{\min})_{p+1} - (b_{\min})_p}{\max\{|(b_{\min})_{p+1} - (b_{\min})_p|\}} \quad (13)$$

Additionally, the calculation for the typical number of sleep mounts is as follows:

$$w = \frac{\sum_{p=1}^t L_r}{t} \quad (14)$$

Where  $t$  is the total number of sleeping mounts, and  $L_r$  stands for sleeping mounts. When the requirements for baby care exchange are satisfied, the DMOA algorithm moves on to the scouting stage.

- (4) A regiment of scouts. Mongooses are at their most sleep-depressed during this stage when families are out on long expeditions. the Scout Mongoose formula is written as (15) Equation

$$s_{p+1} = \begin{cases} s_p - D * \alpha_p * z |s_p - \vec{S}|, & \text{if } w_{p+1} > w_p \\ s_p + D * \alpha_p * z |s_p - \vec{S}|, & \text{Otherwise} \end{cases}$$

Here,  $z$  stands for any number between 0 and 1, and the values of  $D$  and  $S$  are determined using the formulas given.

$$D = \left(1 - \frac{U}{H_U}\right)^{2 * U / H_U}$$

$$\vec{S} = \sum_{p=1}^t \frac{s_p * L_r}{s_p} \quad (16)$$

Babysitters are often young and concentrate daily on triggering female alpha hunting since they are a member of the inferior group. Algorithm 3 displays the R-Lookahead-LSTM-DMOA pseudocode.

- 5) A new evaluation of appropriateness. A solution's viability is assessed using the derived fitness value. In this case, the best answer is the smallest MSE, and the worse options are repeatedly replaced with the better ones.
- (6) SEVERANCE. Until the ideal answer is found, all of the aforementioned stages are carried

#### ALGORITHM 3: Pseudocode of R-Lookahead-LSTM-DMOA

```

Initiate the algorithmic constraints
while (U < HU) do
  For (p = 1 to k) do
    Estimate the fitness of mongoose Set the time counter
    Estimate the value of alpha by equation (5)
    Compute the best solution by equation (6)
    Evaluate the sleeping mound using equation (7)
    Evaluate the mean value of the sleeping mound using equation (8)
    Compute the movement vector using equation (9)
    Execute the scout mongoose for a successive solution using equation (10)
  End for
  
```

c = c + 1  
end while  
Get the best solution

## 5. Results And Discussion

### 5.1. Performance Metrics:

The performance of the suggested model may be assessed using a variety of performance criteria. There are many different metrics for measuring system performance in deep learning. Accuracy, precision, recall, and F1-score are just a few of the performance measures that are covered in the next section.

### 5.2. Accuracy:

Evaluating the accuracy of the algorithm is one technique to determine how frequently a machine learning algorithm accurately classifies data items. The percentage of accurate guesses to all predictions given in equation is this (1).

$$Accuracy = \frac{TP+TN}{TP+TN+FN+FP} \quad (17)$$

### 5.3. Precision:

The percentage of accurate predictions among all inputs is known as accuracy, also known as positive predictive value. Equation can be used to determine accuracy (2).

$$Precision = \frac{TP}{TP+FP} \quad (18)$$

### 5.4. Recall:

Recall, often referred to as sensitivity, refers to the ratio of accurate class predictions to all class inputs. It serves as a gauge for determining how comprehensive the classifier is. Equation can be used to calculate recall (3).

$$Recall = \frac{TP}{TP+FN} \quad (19)$$

### 5.5. F1-Score:

It might be challenging to decide if more precision or lower recall is preferable when comparing different models, or vice versa. The F1 score is the result of combining recall and accuracy. Equation can be used to measure it (20).

$$F1\ Score = 2 \times \frac{Precision \times Recall}{Precision+Recall} \quad (20)$$

True positives, true negatives, false positives, and false negatives are denoted in Equation 1 by the letters TP, TN, FP, and FN, respectively.

The accuracy, recall, and F1-score performance of the suggested models are displayed in Table 1. According to Table 1, the system's total accuracy is

0.987287. The suggested model's recall, and F1 score are 0.986720, and 0.976481, respectively.

**Table 2: LSTM model comparison using various optimization strategies**

Classifiers	Measures			
	Acc	Precis	Recall	F1
LSTM	0.849	0.838	0.834	0.834
RMSp LSTM	0.880	0.885	0.888	0.879
Adam LSTM	0.914	0.910	0.916	0.918
Lookahead-LSTM	0.948	0.946	0.936	0.936
R-Lookahead-LSTM	0.949	0.947	0.937	0.953
Proposed R-Lookahead-DMOA	0.987	0.986	0.986	0.976

**Comparative Analysis of LSTM Models:** Table 2 presents a comprehensive comparison of LSTM models utilizing various optimization strategies. Each model is evaluated based on accuracy, precision, recall, and F1-score. Notably, the proposed R-Lookahead-DMOA optimization strategy outperforms all other models, achieving remarkable results with an accuracy of 0.987287, recall of 0.986720, and F1-score of 0.976481. This performance surpasses all other models, including those implementing LSTM with RMSprop, Adam, RAdam, Lookahead, and R-Lookahead algorithms.

### 5.6. Optimization Algorithm:

In this section, the primary objective is to assess the performance of various optimization techniques, including RMSprop, Adam, RAdam, Lookahead, R-Lookahead-LSTM, and the proposed R-Lookahead-DMOA, using accuracy and loss estimations. The goal is to identify the most suitable optimization method that maximizes accuracy and minimizes loss as the number of iterations progresses. By conducting a thorough analysis, we aim to determine the optimal strategy that ensures rapid convergence, minimized loss,

and enhanced accuracy for our proposed R-Lookahead-DMOA approach in predicting and tackling heart blockage using ECG signal data. Among these optimization techniques, the RAdam algorithm, as an enhancement of Adam, is explored. It incorporates a dynamic adjustment of the adaptive learning rate, allowing it to adapt intelligently to variations in the gradient during training. We assess RAdam's performance over 500 iterations and compare it to the conventional Adam method in terms of accuracy and loss. The Lookahead algorithm, which introduces the concept of maintaining two sets of weights, is also analysed for its impact on convergence speed.

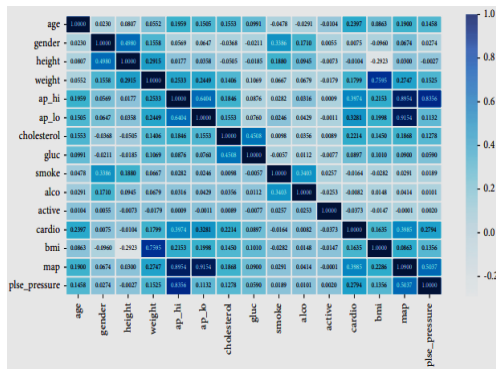


Figure 5: Correlation diagram of characteristic variables

Figure 5 displays a statistical correlation analysis of characteristic variables used for disease prediction. This analysis establishes the relationships between variables such as age, gender, blood pressure, height, weight, glucose, etc. The correlation values are represented in different colors, with black indicating a correlation of 1.0 (positive correlation), blue representing correlations between 0.4 and 0.6 (positive correlation), and white representing no correlation.

Additionally, we investigate the classic Lookahead algorithm in conjunction with the SGD algorithm. This combination shows promising results, characterized by a precision rate of 0.7747 and an error rate of 0.4226. The Stochastic Gradient Descent (SGD) algorithm, known for its efficiency and effectiveness in large-scale optimization tasks, complements the Lookahead algorithm, leading to improved convergence and stable training.

To further enhance the effectiveness of the Lookahead method, we augment it with the RAdam technique. RAdam, an improvement over the conventional Adam algorithm, incorporates a

dynamic adjustment of the adaptive learning rate, allowing it to adapt intelligently to variations in the gradient during training. This enhancement further accelerates the convergence process and results in a reduced loss value of 0.3928.

The combination of Lookahead with SGD and RAdam plays a critical role in our research by improving the performance of the optimization process and enhancing the overall accuracy and efficiency of heart blockage prediction models. This approach demonstrates the synergy between different optimization strategies, creating a robust and powerful optimization framework for our proposed R-Lookahead-DMOA approach.

Therefore, the integration of SGD and RAdam with the classic Lookahead algorithm showcases the significance of exploring hybrid optimization techniques to achieve optimal model performance. This combination contributes to the success of our predictive healthcare application, advancing heart blockage prediction using ECG signal data and paving the way for improved patient care and medical diagnostics.

For a comprehensive understanding of the optimization techniques' comparative performance, we present the precise outcomes of extensive investigation in Tables 3 and 4.

Table 3: Comparison of the optimization methods' accuracy

Optimizers	Accuracy			
	500	1000	1500	2000
RMSprop	0.704	0.715	0.723	0.723
Adam	0.714	0.723	0.736	0.734
RAdam	0.740	0.764	0.747	0.759
Lookahead-LSTM	0.756	0.764	0.768	0.775
R-Lookahead-LSTM	0.763	0.787	0.792	0.806
Proposed R-Lookahead-DMOA	0.848	0.884	0.934	0.980

Table 4: Optimization algorithms' comparison of losses

Optimizers	Loss			
	500	1000	1500	2000
RMSprop	0.574	0.542	0.513	0.495
Adam	0.563	0.519	0.486	0.492
RAdam	0.553	0.482	0.465	0.453
Lookahead-LSTM	0.547	0.458	0.451	0.423

R- Lookahead- LSTM	0.540	0.461	0.428	0.412
ProposedR- Lookahead DMOA	0.523	0.445	0.412	0.369

Therefore, this section provides valuable insights into the strengths and limitations of each optimization algorithm, aiming to identify the optimal strategy that ensures rapid convergence, minimized loss, and enhanced accuracy for our proposed R-Lookahead-DMOA approach in predicting and tackling heart blockage using ECG signal data.

**Discussion**

In the realm of optimization algorithms, several contenders have emerged with their respective strengths and limitations. For example, RMSprop is known for mitigating vanishing and exploding gradients but may face challenges in dealing with complex optimization landscapes, resulting in slower convergence. Adam, on the other hand, boasts rapid convergence and robustness but may struggle with saddle points and require careful hyperparameter tuning. RAdam is an improvement over Adam but may still encounter hurdles with noisy variance estimates.

The Lookahead-LSTM optimization approach shows promise in enhancing training speed and stability but may not completely resolve slow convergence in all situations. Introducing the R-Lookahead-LSTM, a recent advancement in optimization, shows potential in improving convergence rates.

The proposed R-Lookahead-DMOA approach effectively overcomes the limitations of individual optimization techniques by synergistically integrating RAdam, Lookahead, and LSTM. The dynamic learning rate in R-Lookahead-DMOA ensures adaptive and efficient gradient adjustment, leading to swifter convergence and optimized model performance. The approach also mitigates the slow convergence issue observed in classical Lookahead algorithms, resulting in

improved training stability and reduced mean loss values.

**6. Conclusions**

The R-Lookahead-LSTM-DMOA approach presented in this study demonstrates significant advancements in heart blockage prediction using ECG signal data. The proposed technique surpasses existing optimization algorithms, providing accurate and efficient disease prediction models. With an impressive accuracy rate of 0.987287, recall of 0.986720, and F1-score of 0.976481, the proposed approach outperforms various other optimization strategies and conventional LSTM models. The versatility and adaptability of the R-Lookahead-DMOA approach make it a promising optimization strategy for predictive healthcare applications. While the results are promising, there is potential for further advancements through hybrid optimization schemes and incorporating additional indicators and data sources for cardiac classification. Continued research and refinement will contribute to refining the model's performance, making it a reliable tool in predictive healthcare with potential transformative applications in medical diagnostics, leading to enhanced patient care and improved healthcare efficiency

**Declarations**

**-Availability of data and materials**

All data generated or analysed during this study are included in the article.

**-Competing Interests**

The authors declare that they have no conflict of interest.

**-Funding**

This research received no specific grant from any funding agency in the public, commercial, or not-for-profit sectors.

**List of Abbreviations**

S.No	Algorithm	Abbreviations
1.	LSTM	Long Short Term Memory
2.	DMOA	Dwarf Mongoose Optimization
3.	BF-PSO	Bacterial Foraging Particle Swarm Optimization
4.	BFO	Bacterial Foraging Optimization
5.	Bi-LSTMCRF	Bidirectional long short-term memory Conditional Random Field
6.	RLNNC	regression learning-based neural network classifier
7.	MSSO	Modified Sarp Group Optimization
8.	ANFIS	Adaptive Neuro-Fuzzy Inference System
9.	BP	blood pressure
10.	RMSprop	Root Mean Square propagation
11.	OCD	Obsessive-Compulsive Disorder
12.	UCI	Ultrasonic Contact Impedance
13.	SGD	Stochastic gradient descent
14.	RAadam	<b>Random</b> encoding of Aggregated Deep Activation Maps

**References**

- [1] X. Hu, C. Jin, A. Mamoun et al., "On the design of block chain based ECDSA with fault-tolerant batch verification protocol for block chain-enabled IoMT," *IEEE Journal of Biomedical and Health Informatics*, vol. 12, no. 3, pp. 23–56, 2021.
- [2] W. Wang, C. Qiu, Z. Yin et al., "Block chain and PUF-based light weight Authentication protocol for wireless medical sensor networks," *IEEE Internet of @ings Journal*, vol. 34, no. 2, 2021.
- [3] M. Kukar, I. Kononenko, C. Grošelj, K. Kralj, and J. Fettich, "Analysing and improving the diagnosis of ischaemic heart disease with machine learning," *Artificial Intelligence in Medicine*, vol. 16, no. 1, pp. 25–50, 1999.
- [4] Y. S. Kim, S. Y. Sohn, and C. N. Yoon, "Screening test data analysis for liver disease prediction model using growth curve," *Biomedicine & Pharmacotherapy*, vol. 57, no. 10, pp. 482–488, 2003.
- [5] C. M. Chu, H. J. Tscai, N. F. Chu et al., "The establishment of bayesian coronary artery disease prediction model," in *Proceedings of the AMIA Annual Symposium Proceedings American Medical Informatics Association*, pp. 925–930, Qazvin, Iran, 2005.
- [6] M. Green, J. Bjork, J. Forberg, U. Ekelund, L. Edenbrandt, and M. Ohlsson, "Comparison between neural networks and multiple logistic regression to predict acute coronary syndrome in the emergency room," *Artificial Intelligence in Medicine*, vol. 38, no. 3, pp. 305–318, 2006.
- [7] D. Yao, J. Yang, and X. Zhan, "A novel method for disease prediction: hybrid of random forest and multivariate adaptive regression splines," *Journal of Computers*, vol. 8, no. 1, pp. 170–177, 2013.
- [8] S. Elango and J. Sundararajan, "MNN: Multiclass neural network classifier for cardiac disease prediction models," *Asian Journal of Research in Social Sciences and Humanities*, vol. 6, no. 1, pp. 293–309, 2016.
- [9] S. Patidar, R. B. Pachori, and U. Rajendra Acharya, "Automated diagnosis of coronary artery disease using tunable-Q wavelet transform applied on heart rate signals," *Knowledge Based Systems*, vol. 82, pp. 1–10, 2015.
- [10] T. Zeng and Y. Zhang, "Medical data analysis and disease prediction model based on support vector machine," *Journal of Medical Imaging and Health Informatics*, vol. 6, no. 4, 2016.
- [11] Dr. S. Vijayalakshmi. Early detection of breast cancer using robust back propagation neural network classifier. *Rom Biotech nollett*. 2022; 27(2): 3407-3415 DOI: 10.25083/rbl/27.2/3407.3415
- [12] Annamalai, Manikandan & Muthiah, Ponni. (2022). An Early Prediction of Tumor in Heart by Cardiac Masses Classification in Echocardiogram Images Using Robust Back Propagation Neural Network Classifier.

- Brazilian Archives of Biology and Technology. 65. 10.1590/1678-4324-202210316.
- [13] Manikandan, Annamalai, M, PonniBala. (2022). Intracardiac Mass Detection and Classification Using Double Convolutional Neural Network Classifier. *Journal of Engineering Research*. 65. <https://doi.org/10.36909/jer.12237>
- [14] Sheikdavood K, Surendar P, Manikandan A. Certain Investigation on Latent Fingerprint Improvement through Multi-Scale Patch Based Sparse Representation. *Indian Journal of Engineering*. 2016; 13(31):59-64.
- [15] S. Dhanasekaran, Dr. P. Mathiyalagan, Rajeshwaran, A. Manikandan, "Automatic Segmentation of Lung Tumors Using Adaptive Neuron-Fuzzy Inference System ", *Annals of RSCB*, pp. 17468–17483, Jun. 2021
- [16] Manikandan, A., & Sakthivel, J. (2017a). Recognizable Proof of Biometric System With Even Distorted And Rectification States. *Journal of Advanced Research in Dynamical and Control Systems*, 9(2), 1393–1398.
- [17] Manikandan, A., & Jamuna, V. (2017). Single Image Super Resolution via FRI Reconstruction Method. *Journal of Advanced Research in Dynamical and Control Systems*, 9(2), 23–28.
- [18] Manikandan, A., Suganya, K., Saranya, N., Sudha, V., & Sweetha, S. (2017). Assessment of Intracardiac Masses Classification. *Journal of Chemical and Pharmaceutical Sciences*, 5, 101–103.
- [19] Ashokkumar, N. & Meera, S. & Anandan, P. & Murthy, Mantripragada & K S, Kalaivani & Alahmadi, Tahani & Alharbi, Sulaiman & Raghavan, S. & Jayadhas, s. (2022). Deep Learning Mechanism for Predicting the Axillary Lymph Node Metastasis in Patients with Primary Breast Cancer. *BioMed Research International*. 2022. 10.1155/2022/8616535.
- [20] K. N. R. C. K. D. D. T. "Survey on 2D-DCT Based Image Watermarking With High Implanting Limit and Robustness". *International Journal on Recent and Innovation Trends in Computing and Communication*, vol. 4, no. 10, Oct. 2016, pp. 161-4, doi:10.17762/ijritcc.v4i10.2576.
- [21] Karpagalakshmi, RC, Tensing, D & Kalpana, A.M. (2016). Image Localization using Deformable Model and its Application in Health Informatics. *Journal of Medical Imaging and Health Informatics*, vol. 6(8), pp. 1972  
1976. <https://doi.org/10.1166/jmihi.2016.1959>.
- [22] Namrata, K, Karpagalakshmi, R, C, Manikandasaran, S, S. (2017). Implementation of Novel Technique for Image Watermarking Using 2D-DCT. *International Journal of Pure and Applied Mathematics*, volume 117(16), pp. 221-226.
- [23] T. Ramalingam, R. Umamaheswari, R. C. Karpagalakshmi, K. Chandramohan, M. S. Sabari. (2021). Location of plant Leaf maladies utilizing picture division. *Journal of Image processing and Artificial Intelligence*. vol. 7(3). <http://dx.doi.org/10.46610/JOIPAI.2021.v07i03.002>.
- [24] Gopalan, S. H., Vignesh, V., Mahendran, N., & Dinesh, M. T. P. P. (2021). Dynamic Clinical Trials Management in Anunreliable Environment using Blockchain. *Design Engineering*, 817-822.
- [25] D. S. S, N. H. A. Rufus, D. Anand, R. S. Rama, A. Kumar and A. S. Vigneshwar, "Evolutionary Optimization with Deep Transfer Learning for Content based Image Retrieval in Cloud Environment," 2022 International Conference on Augmented Intelligence and Sustainable Systems (ICAISS), Trichy, India, 2022, pp. 826-831, doi: 10.1109/ICAISS55157.2022.10011122
- [26] Khan, Ali Haider; Hussain, Muzammil (2021), "ECG Images dataset of Cardiac Patients ", Mendeley Data, V2, doi: 10.17632/gwbz3fsgp8.2
- [27] Sobahi, N., Sengur, A., Tan, R., & Acharya, U. R. (2022). Attention-based 3D CNN with residual connections for efficient ECG-based COVID-19 detection. *Computers in Biology and Medicine*, 143, 105335. <https://doi.org/10.1016/j.compbiomed.2022.105335>